

# Role of phason defects on the conductance of a one-dimensional quasicrystal

K. Mouloupoulos and S. Roche

*Laboratoire d' Etudes des Propriétés Electroniques des Solides, CNRS, 38042 Grenoble, France*

(Received 9 May 1995)

We have studied the influence of a particular kind of phason defect on the Landauer resistance of a Fibonacci chain. Depending on parameters, we sometimes find the resistance to decrease upon introduction of defect or temperature, a behavior that also appears in real quasicrystalline materials. We demonstrate essential differences between a standard tight-binding model and a full continuous model. In the continuous case, we study the conductance in relation to the underlying chaotic map and its invariant. Close to conducting points, where the invariant vanishes, and in the majority of cases studied, the resistance is found to decrease upon introduction of a defect. Subtle interference effects between a sudden phason change in the structure and the phase of the wave function are also found, and these give rise to resistive behaviors that produce exceedingly simple and regular patterns.

## I. INTRODUCTION

According to recent experiments,<sup>1</sup> quasicrystals have curious (for metallic materials) transport properties. For example, anomalously high values of the low-temperature resistivity have been reported, and the resistivity goes down with introduction of defects or with increase of temperature. The anomalously high resistivity has been partly accounted for by the existence of a pseudogap at the Fermi energy. For the temperature or defect dependence there is no clear consensus yet. In numerical simulations of two-dimensional (2D) systems, fluctuating behavior for the resistance of a system with defects (with *random* disorder) with respect to that of a pure system is observed, namely the resistivity can either go up or down.<sup>2</sup>

Here we attempt to address these behaviors for a 1D system by focusing on the electronic *phase relations* in real space that actually determine the conductance. We study, for example, the scattering of electrons on a quasiperiodic (Fibonacci) arrangement of  $\delta$ -function potentials (a continuous model with the full phase coherence included). After determining the Landauer conductance of a finite part of such a system, then we introduce a particular type of defect of a step form in hyperspace<sup>3</sup> (called “phason defect” from now on) and we study how this defect *influences those phase relations*. This is therefore a study of the effect of an abrupt “phase” change in the structure (with “phase” defined in hyperspace) on the phase coherence of the electronic wave function in real space (with phase defined in the usual quantum-mechanical way). [The role of the initial “phase” of pure chains (without defects) on the resistance has been studied by other authors.<sup>4</sup>]

The quasicrystalline structure can induce exotic (“critical”) states<sup>5</sup> that are intermediate between localized and extended states. Especially in the case of a chain with  $\delta$  potentials with positions or strengths arranged in a pure Fibonacci sequence, all states are critical independent of values of parameters.<sup>6</sup> One consequence that we observe, for a *finite* part of the Fibonacci chain, is a rather unpredictably fluctuating variation of the Landauer resistance with the length of the sample<sup>7</sup> (except when we are on special energy-regions

of integrability, as we will see below). But in addition to this irregular variation for a pure Fibonacci chain, we here also attempt a study of the variation of the Landauer resistance for the system with a phason defect as well, both with respect to the length of the sample and also with respect to the position of the defect. The comparison of the resistances between the pure system and the system with the defect shows some interesting regular patterns, provided that we are close to special points associated with the vanishing of the invariant  $I$  of the underlying dynamical map<sup>5</sup> (on which points, both problems are integrable). In addition, in the majority of values of the parameters, the pure system is found to be more resistive than the one with the defect.

It is also demonstrated that our use of a continuous model is critical in obtaining our results. As we show, these results would have actually been missed had one first made a tight-binding approximation (i.e., keeping only nearest-neighbor overlaps). Our work is therefore a concrete example of the danger<sup>8</sup> that the usual discretized approximations incorporate, especially when systems with quasiperiodicity are considered, where subtle interference effects between the phase of the wave functions and the “phase” in hyperspace can be expected.

## II. A TIGHT-BINDING MODEL

Let us first use a tight-binding model, in order to compare with the fuller treatment that is given later in Sec. III. We analyze the standard scattering problem by connecting an outside conductor (simulated by a simple periodic chain) to the left and to the right of our finite system. We then study the scattering of an electron coming from the left with a wave vector  $k$ , and we determine the Landauer resistance<sup>9</sup> of our finite system (ratio of the reflection to the transmission coefficient). The method used for this is the standard transfer matrix method.<sup>7</sup>

The Hamiltonian for a general (mixed) tight-binding model is

$$H = \sum_n \epsilon_n |n\rangle \langle n| + t_n (|n\rangle \langle n+1| + |n+1\rangle \langle n|) \quad (1)$$



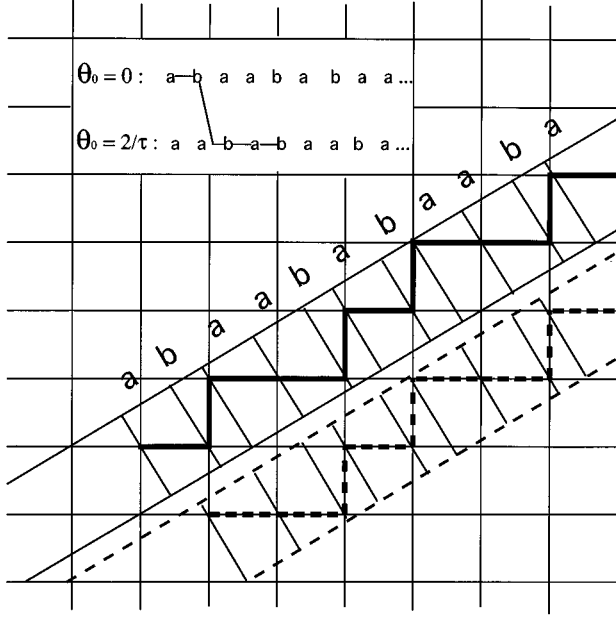


FIG. 1. Hyperspace construction of the standard Fibonacci chain (top) and a  $2/\tau$  shifted chain (bottom) ( $2/\tau$  is the “initial phase”).  $\theta_0$  (in units where the width of the window is 1) and it is equal to the displacement of the physical line in the perpendicular direction. The resulting chains, as well as the way that the defect is introduced, are illustrated on the top left, through a step modification of the physical line.

For large values of  $N$  we get 50% of this favorable behavior. (We have also carried out cases of sequences<sup>11</sup> with many defects, where we also find irregularly fluctuating behavior, but with the *scale* of fluctuations being much higher.)

### III. CONTINUOUS SCHRÖDINGER EQUATION MODELS

In this continuous case, which has the advantage of not suffering from truncation approximations, the matrix form of the Schrödinger equation results from matching wave functions and derivatives at scattering points. This yields a generalized Poincaré map<sup>12</sup> of the following form

$$\begin{pmatrix} \Psi_{n+1} \\ \Psi_n \end{pmatrix} = M_n \begin{pmatrix} \Psi_n \\ \Psi_{n-1} \end{pmatrix} \quad (5)$$

with

$$M_n = \begin{pmatrix} K_{11}(n+1) + K_{22}(n) & \frac{K_{12}(n+1)}{K_{12}(n)} & -\frac{K_{12}(n+1)}{K_{12}(n)} \\ 1 & & 0 \end{pmatrix}. \quad (6)$$

In the special case of a scattering potential of the form  $V(x) = \sum_n \lambda_n \delta(x - x_n)$  and with  $k = \sqrt{2mE/\hbar^2}$  one obtains<sup>13</sup>

$$K_{11}(n+1) = \text{cosk}(x_{n+1} - x_n) + \frac{\lambda_n}{2k} \frac{2m}{\hbar^2} \text{sink}(x_{n+1} - x_n),$$

$$K_{12}(n+1) = \frac{\text{sink}(x_{n+1} - x_n)}{k},$$

$$K_{22}(n+1) = \text{cosk}(x_{n+1} - x_n) + \frac{\lambda_{n+1}}{2k} \frac{2m}{\hbar^2} \text{sink}(x_{n+1} - x_n). \quad (7)$$

#### A. Comparison with Sec. II

Let us pause for a moment to see how a tight-binding approximation is usually derived. To change to a localized description one typically writes the wave function  $\Psi(x)$  in terms of localized states  $\phi_n$ , namely  $\Psi(x) = \sum_n C_n \phi_n(x - x_n)$  with  $\phi_n(x - x_n) = \sqrt{\lambda_n} e^{-\lambda_n |x - x_n|}$  and then neglects the overlap between distant  $\phi_n$ 's; assuming that only nearest-neighbor overlaps are significant one obtains a tight-binding model with site and hopping elements<sup>14</sup>

$$\epsilon_n = -\frac{1}{2} \lambda_n^2$$

$$t_{n,n\pm 1} = -\sqrt{\lambda_n^3 \lambda_{n\pm 1}} e^{-\lambda_{n\pm 1} |x_{n\pm 1} - x_n|}. \quad (8)$$

It is important to note then that in the special case of a continuous model with identical strengths  $\lambda$  and quasiperiodic arrangements ( $\Delta x$ 's taking two values in a Fibonacci sequence), which we later analyze in detail (see Sec. III B), we would just obtain a simple off-diagonal tight-binding approximation (since in this case all the  $\epsilon_n$  are identical). This demonstrates a deficiency of the tight-binding approximation, on which we now elaborate.

In the case of Fibonacci arrangements (let us say of both  $\epsilon$ 's and  $t$ 's and for  $N = F_n$  (a Fibonacci number) we have in the tight-binding approximation [with definitions  $P_n \equiv M_{F_n} \cdots M_1$ , with  $M$ 's given in (2)] the well-known<sup>5</sup> recursive scheme  $P_{n+1} = P_{n-1} \cdot P_n$ , with starting matrices

$$P_1 = \begin{pmatrix} \frac{E - \epsilon_a}{t_a} & -1 \\ 1 & 0 \end{pmatrix},$$

and

$$P_2 = \begin{pmatrix} \frac{E - \epsilon_a}{t_a} & -\frac{t_b}{t_a} \\ 1 & 0 \end{pmatrix} \begin{pmatrix} \frac{E - \epsilon_b}{t_b} & -\frac{t_a}{t_b} \\ 1 & 0 \end{pmatrix}$$

and hence the usual trace map<sup>5</sup>  $x_{n+1} = 2x_n x_{n-1} - x_{n-2}$  [with the definition  $x_n = \frac{1}{2} \text{tr}(P_n)$ ]. This map has the well-known invariant  $I = x_{n+1}^2 + x_n^2 + x_{n-1}^2 - 2x_{n+1}x_nx_{n-1} - 1$ . Straight-forward evaluation for the above case yields

$$I = \frac{1}{4} \left[ (\epsilon_a - \epsilon_b) \left( \frac{E - \epsilon_b}{t_b^2} - \frac{E - \epsilon_a}{t_a^2} \right) + \left( \frac{t_a}{t_b} - \frac{t_b}{t_a} \right)^2 \right]. \quad (9)$$

In our case of a simple off-diagonal model (i.e.,  $\epsilon_a = \epsilon_b$ ) [but also for the case of diagonal models (i.e.,  $t_a = t_b$ )]  $I$  is  $E$  independent as seen from (9), always positive, and it never

vanishes. This is a deficiency of the approximation, as discussed below. (Note that even in the case of a mixed model, where  $I$  vanishes only for a single value of  $E$ , the elementary matrices  $M$  do *not* commute at this value, which is a major difference with the full continuous model, as will be discussed in Sec. III B).

We will see below that, because of implicit truncation errors, the tight-binding models miss interesting patterns associated with the *zeros* of the invariant  $I$  of the underlying dynamical map, where the basic matrices commute. These are actually relevant to conduction and are treated next (in Sec. III B) in the continuous Schrödinger formulation.

### B. Example: Periodic system

Let us first discuss a problem where the scattering potential is an array of equally-spaced (with length  $a$ )  $\delta$  functions of equal strengths ( $\lambda$ ). Then, again two cases appear naturally (we take  $2m/\hbar^2=1$ , or, equivalently, replace everywhere  $k$  by  $k*\hbar^2/2m$  in what follows):

$$(a) \quad \text{For } \left| \cos ka + \frac{\lambda}{2k} \sin ka \right| < 1$$

$$\Rightarrow \left( \frac{\mathcal{R}}{\mathcal{T}} \right) = \left( \frac{\lambda}{2k} \right)^2 \frac{\sin^2 N\phi}{\sin^2 \phi}$$

with  $\phi$  defined by  $\cos \phi = \cos ka + (\lambda/2k) \sin ka$  [which is seen to be the same as in the usual treatment of the Krönig-Penney model<sup>15</sup> for the case of allowed bands (for  $N \rightarrow \infty$ )]. We note again the oscillatory behavior of the resistance with length.

It is easy to show that the naturally appearing phase  $\phi$  determines the crystal momentum  $q$  through  $\phi = qa$  (with such an identification, the resulting wave functions indeed satisfy the Bloch theorem, as can be easily checked). We can also see that the zeros of  $(\mathcal{R}/\mathcal{T})$  determine the allowed values of  $q$  (from band theory) for the *infinite* periodic system. This is an important point, because it motivates our later treatment of a Fibonacci problem, where we will enforce the vanishing of the resistance in order to simulate the thermodynamic limit:

$$(b) \quad \text{For } \left| \cos ka + \frac{\lambda}{2k} \sin ka \right| > 1$$

$$\Rightarrow \left( \frac{\mathcal{R}}{\mathcal{T}} \right) = \left( \frac{\lambda}{2k} \right)^2 \frac{\sinh^2 N\phi}{\sinh^2 \phi}$$

with  $\phi$  defined by  $\cosh \phi = \cos ka + (\lambda/2k) \sin ka$ . This corresponds to the case of gaps in the limit  $N \rightarrow \infty$ . Indeed the resistance grows exponentially as  $N \rightarrow \infty$ . In this case, wave functions decrease with a characteristic length  $\Lambda = 2aN / [\ln(1 + \mathcal{R}/\mathcal{T})]$ .

Once again the study of complex unit cells is of course possible. Also the introduction of a single defect results in interference effects that can be easily studied through this method.

### C. Schrödinger equation with $\delta$ potentials in Fibonacci and in phason-defect sequence

In the pure case a recursive procedure of the form  $P_{n+1} = P_{n-1} \cdot P_n$  can also be established for this case (with starting matrices depending on the description). For example, in the case of equally spaced (a)  $\delta$  potentials with  $\lambda_n = \{\lambda_a, \lambda_b\}$  in Fibonacci arrangement, a natural description is the one given in the previous section (in terms of matrices  $M_n$ ) (with  $P_n = M_{F_n} \cdots M_1$ ). Then the invariant is

$$I = \frac{(\lambda_a - \lambda_b)^2 \sin^2(ka)}{4k^2}$$

i.e.,  $I \geq 0$ . [Its zeros constitute a periodic pattern  $k_s = n\pi/a$ , ( $n \neq 0$ ).]

*Our system.* The system, however, we will analyze in detail corresponds to  $\delta$  potentials with equal strengths ( $\lambda$ ) but quasiperiodic arrangements  $\{(x_n - x_{n-1})\} = \{a, b\}$  in Fibonacci arrangement,<sup>16-18</sup> as already mentioned earlier. In this case, an alternative description (in terms of the coefficients  $A_n$  and  $B_n$  of the two linearly independent plane waves in the region between two  $\delta$  potentials) is more natural. One obtains<sup>16</sup>

$$\begin{pmatrix} A_{n+1} \\ B_{n+1} \end{pmatrix} = \Lambda(n) \cdot \begin{pmatrix} A_n \\ B_n \end{pmatrix} \quad (10)$$

with

$$\Lambda(n) = \begin{pmatrix} \left(1 - \frac{i\lambda}{2k}\right) e^{ik(x_{n+1} - x_n)} & -\frac{i\lambda}{2k} e^{ik(x_{n+1} - x_n)} \\ \frac{i\lambda}{2k} e^{-ik(x_{n+1} - x_n)} & \left(1 + \frac{i\lambda}{2k}\right) e^{-ik(x_{n+1} - x_n)} \end{pmatrix} \quad (11)$$

for  $\delta$  potentials (once again we have set  $2m/\hbar^2=1$ ). In this description the Landauer resistance is given again by  $\mathcal{R}/\mathcal{T} = |P_{12}|^2$  with  $P$  the product of  $\Lambda$ 's, namely  $P_n = \Lambda(F_n) \cdots \Lambda(1)$ . In this case the invariant  $I$  of the underlying dynamical map turns out to be<sup>19</sup>  $I = \lambda^2 \sin^2 k(a-b)/4k^2$ , i.e., also  $I \geq 0$ . Its zeros now constitute a periodic pattern  $k_s = n\pi/(a-b)$  and will be the focus of our work in what follows.

These special points  $k_s$  are missed in the corresponding tight-binding model, as we showed earlier. In the present continuous model they turn out to correspond to commuting consecutive matrices, i.e.,  $[P_{n+1}, P_n] = 0$  [which is consistent with the known relation<sup>8</sup>  $4I + 2 = \text{tr}(P_n \cdot P_{n+1} \cdot P_n^{-1} \cdot P_{n+1}^{-1})$ ], but even stronger, they lead to commuting elementary matrices (11). Indeed, it turns out that their commutator is

$$[\Lambda(\Delta x = a), \Lambda(\Delta x = b)] = \lambda \frac{e^{ik(a-b)}}{4k^2} (1 - e^{2ik(b-a)})$$

$$\times \begin{pmatrix} \lambda & \lambda - 2ik \\ -\lambda - 2ik & -\lambda \end{pmatrix} \quad (12)$$

which vanishes for all special points  $k = \{k_s\}$ .

One can therefore say that, from a conduction point of view, the problem looks formally similar to a periodic problem. This is more concretely described through the following properties of the special points  $\{k_s\}$ :

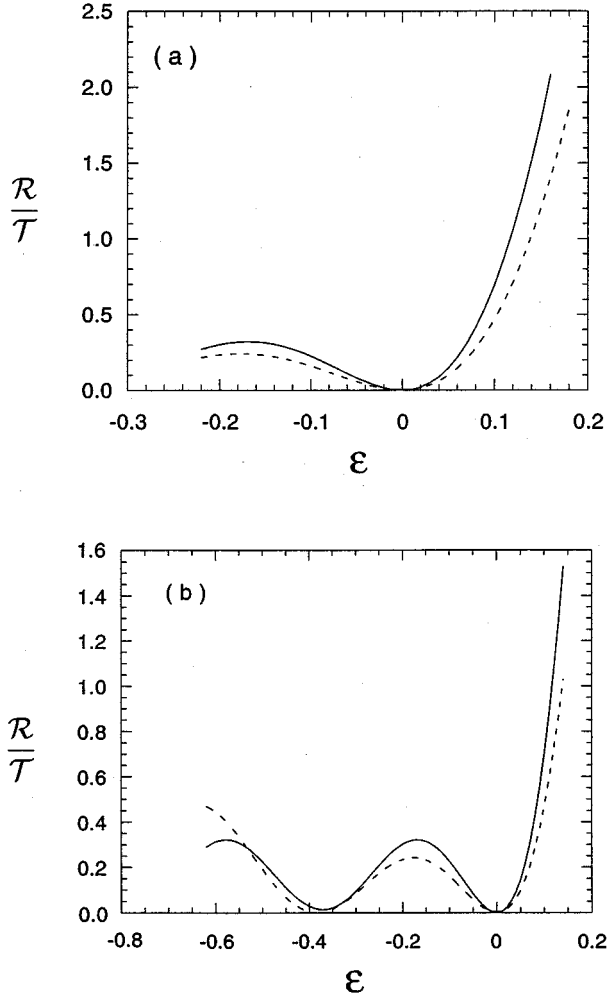


FIG. 2. (a) Typical local behavior of the Landauer resistance of the chain with a defect (dashed line) compared to a pure chain (solid line), around a special point. (Horizontal axis is  $k$  space, with  $k = k_s + \epsilon$ ). In the case of the defect, it rises from zero *lower* than the pure system. (b) The same behavior but in a more extended region of  $k$  space, showing various crossovers, corresponding to chaotic behavior shown in Fig. 8(c).

(1) They are the conducting points (extended states) surviving<sup>16</sup> in the limit  $N \rightarrow \infty$ .

(2) The Landauer resistance can be written *exactly* in closed form for  $k = \{k_s\}$ , and the expression looks like that of a periodic system (see below).

(3) The set of points  $k_s$  is robust<sup>8</sup> against disorder (essentially because of the above mentioned commutations). In fact it exists either for a periodic or for a random system (of two letters).

In what follows, we focus on these points  $k_s = n\pi/(a-b)$  with  $a = \tau = (1 + \sqrt{5})/2$ ,  $b = 1$  (Fibonacci chain): Exactly on those points we get the Landauer resistance in closed form (for the Fibonacci or any disordered system of  $\{a, b\}$ ):

$$\left. \frac{\mathcal{R}}{\mathcal{T}} \right|_{k=k_s} = \left( \frac{\lambda}{2k_s} \right)^2 \frac{\sin^2 N\phi}{\sin^2 \phi} \quad (13)$$

with  $\phi$  defined by  $|\cos \phi| = |\cos k_s a + (\lambda/2k_s) \sin k_s a| = |\cos k_s b + (\lambda/2k_s) \sin k_s b|$  (for  $2m/\hbar^2 = 1$ ).

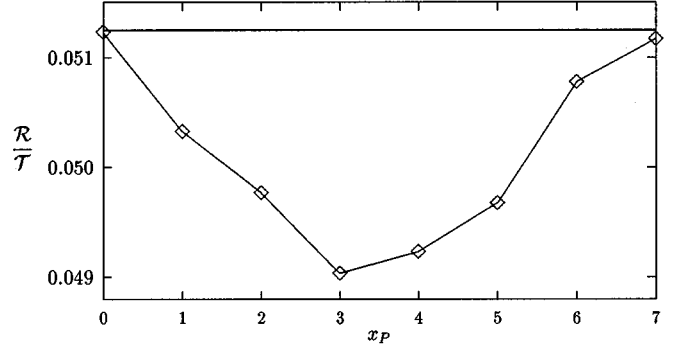


FIG. 3. Comparison between resistances of a pure small chain ( $N=34$ ) and all possible chains with a defect of the same length, for a fixed  $k$  close to a special point ( $k = k_s + \epsilon$ ). Numbers from 0 to 7 correspond to the eight possible chains with the defect (0 corresponding to the defect being closer to the left end, and 7 to the defect being closer to the right end of the chain). We note a simple behavior with the defect position ( $x_P$ ) and a resistance that is always lower than that of the pure chain (horizontal line). This simple (but discrete and asymmetric) behavior becomes smooth and symmetric for long chains (see Fig. 4) where  $x_P$  becomes quasicontinuous. We have chosen  $\epsilon = 10^{-4}$  (in units  $b=1$ ).

Motivated by our earlier discussion on a finite piece of a periodic system (where we saw that the values of  $k$  that made the oscillating resistance *vanish* correspond to the allowed states of the *infinite* system), we now *enforce* a conducting behavior (resonance): For any fixed  $N$ , we choose  $\lambda$  in such a way as to have a vanishing resistance (exactly at  $k = k_s$ ), namely  $(\mathcal{R}/\mathcal{T})|_{k=k_s} = 0$  (for *both* the pure Fibonacci and the system with the defect). (This gives the representative behavior in the thermodynamic limit where this vanishing is actually expected for  $k = k_s$  and for any  $\lambda$ ; see below). As a consequence we get  $(N-1)$  different appropriate values of  $\lambda$  (both positive and negative) given by

$$\lambda_s = \frac{2k_s(\cos \phi_s - \cos k_s b)}{\sin k_s b} \quad (14)$$

with the internal phase  $\phi_s$  defined by  $\phi_s = m\pi/N$  with  $m = 1, \dots, N-1$  that correspond to vanishing  $(\mathcal{R}/\mathcal{T})|_{k=k_s}$ . The  $(N-1)$  values of the phase  $\phi_s$  are symmetrically placed around  $\pi/2$  and as  $N$  increases they cover densely the entire upper half of the trigonometric circle. Consequently, the vanishing of  $(\mathcal{R}/\mathcal{T})|_{k=k_s}$  is representative of the behavior in the thermodynamic limit for *any* arbitrary value of  $\lambda$ , and that is the reason we enforce it even for a finite system. By doing so, we then study the behavior *around* the conduction points  $k_s = n\pi/(\tau-1)$ . Below we summarize our results on the behavior of the resistance, of both the pure and the system with the defect, as  $k$  varies in the local neighborhood of the conduction points  $k_s$ .

### 1. Smallest system (consistent with boundary conditions): $N=5$

The results are given in Fig. 2, where we show the local regions around the lowest conducting point ( $n=1$ ) for one value of  $\phi_s$ , showing that the resistance of the system with the defect *always rises lower* than the one of the pure system

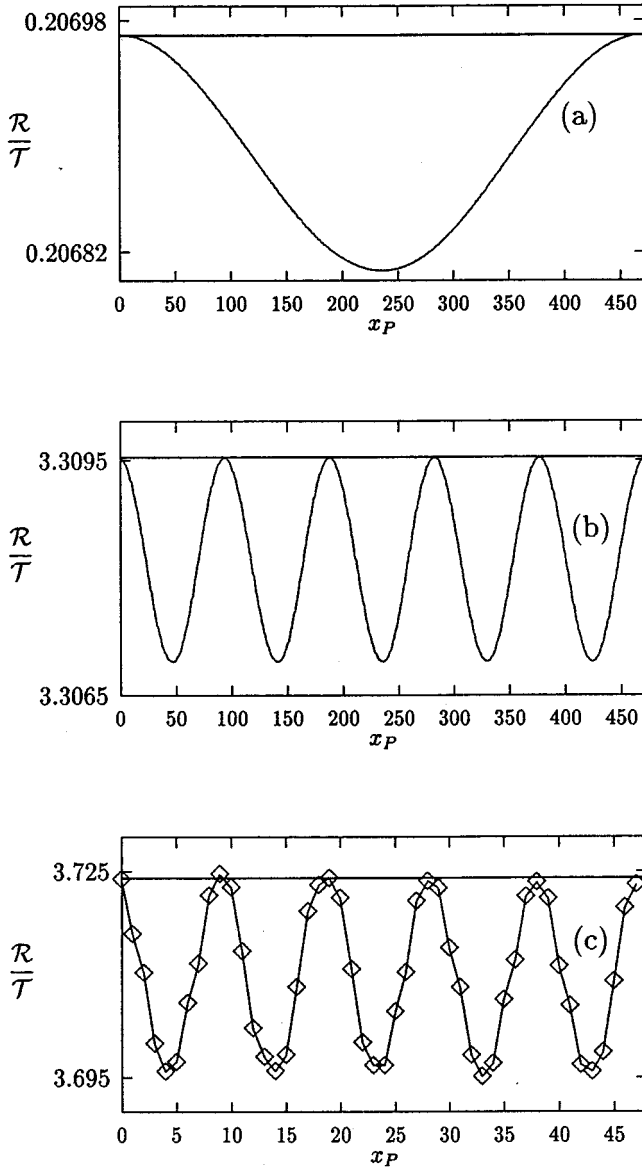


FIG. 4. Corresponding results for long chains (a) for  $N=2000$  the simplest possible pattern appears for  $\phi_s = \pi/N$ , and it is a smooth and symmetric analog of Fig. 3. This is always the pattern appearing for any  $N$  (and  $m=1$ ). It also turns out that all the chains with a defect are always less resistive than the pure one (horizontal line). We have taken  $\epsilon=10^{-9}$ . (b) Corresponding result for  $m=5$ . Again, a simple oscillatory pattern appears (with the number of bumps equal to  $m$ ), which is generally valid for small  $m$ 's. These simple patterns are quasicontinuous analogs of asymmetric and discrete patterns that are found for small chains, as shown in (c) which corresponds to  $N=200$ .

(this is also true for any  $\phi_s$ ). We also show the complicated behavior of the Landauer resistance in more extended regions around a special point and for one particular  $\phi_s$ .

Of course the problem is analytically solvable. By way of an example we give the analytical solution for  $n=1$  [ $k_s = \pi/(\tau-1)$ ],  $m=1$  ( $\phi_s = \pi/5$ ) which is

$$\left. \frac{\mathcal{R}}{\mathcal{T}} \right|_{\text{pure}} = 45.3087 \left( k - \frac{\pi}{\tau-1} \right)^2 + \dots,$$

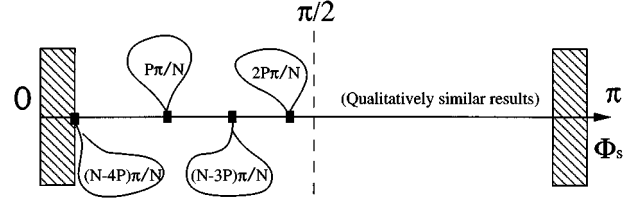


FIG. 5. Global view of the resistive behavior in  $\phi_s$  line. See text for details (end of Sec. III). Shaded areas show regions of values of  $\phi_s$  (and correspondingly of the potential strength parameter  $\lambda$ ) where the resistive behavior is very simple. The following three loops show the places where one recovers simple resistive patterns and transitions in the resistive behavior.

$$\left. \frac{\mathcal{R}}{\mathcal{T}} \right|_{\text{defect}} = 30.7868 \left( k - \frac{\pi}{\tau-1} \right)^2 + \dots.$$

This is the typical behavior for *all* points examined ( $1 \leq n \leq 5$ , all  $m$ 's) i.e., the Landauer resistance of the system with the phason defect around the conducting points  $k_s$ , rises (from zero) *always lower* than the corresponding one for the pure system.

## 2. $N=13$

Extensive numerical results have been obtained in this case, where we have three possible systems with this type of defect, for  $1 \leq n \leq 5$  and for all 12 phases  $\phi_s$ . Out of those 12 cases, in eight of them *all* three systems with defect have Landauer resistances *lower* than that of the pure system. In only two cases one sequence with defect rises slightly higher and also in two other cases another sequence also rises slightly higher than the pure system. We call these few cases (where the system with the defect is more resistive) “unfavorable cases.”

## 3. Long chains

We have carried out numerical calculations on chains up to more than 3000 sites, taking as a numerical convergence criterium the unitarity condition of our total transfer matrices. Because of the full phase coherence, the transmission behavior of the chains with a defect depends on the discrete position  $xp$  of the defect in interesting ways. In long chains the variable  $xp$  becomes quasicontinuous, and the discrete and asymmetric patterns found for small chains [see, for example, Figs. 3 and 4(c)], now appear smooth and symmetric [Figs. 4(a) and 4(b)]. Moreover, their actual form depends on the value of  $\phi_s$ , which can be considered as a discrete label parametrizing the family of potential strengths  $\lambda$  that enforce vanishing of resistance on special points. The results show interesting patterns summarized below and shown pictorially in Fig. 5.

We observe a symmetry in the qualitative behavior around the value  $\phi_s = \pi/2$  (although the values of  $\lambda$  corresponding to symmetric values of  $\phi_s$  are always different) as seen from Eq. (14). Up to this symmetry, we also observe a type of recurrent simplicity in the resistive behavior of the system with the defect, which we loosely call “cyclic” (with period  $P$ ). For small to medium values of  $\phi_s$ , in more detail, for

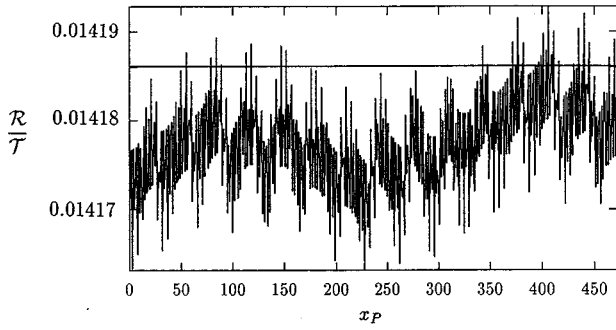


FIG. 6. Modulated resistive behaviors for  $m$  between  $N-4P$  and  $P$ . The system with a defect is, in the majority of cases, less resistive than the pure one (horizontal line).

$m < N-4P$ , with  $m$  defined by  $\phi_s = m(\pi/N)$  and with  $P$  being the number of possible defect-points (note that for a given chain-length  $N$  there is a unique  $P$  always satisfying the inequality  $N < 5P$  for any  $N > 5$ ), we observe *exceedingly* simple oscillatory patterns (examples are shown in Fig. 4). Furthermore, we observe that in these cases the system with the defect is *always* less resistive than the pure one. A qualitatively similar behavior is observed in the mirror symmetric region (see the two shaded regions in Fig. 5). It is interesting to point out that the above “favorable” behavior is valid for sufficiently strong absolute values of  $\lambda$ , namely  $|\lambda| \geq \lambda_0$  with

$$\lambda_0 = \frac{2\pi}{\tau-1} \frac{\left| \cos\left(\frac{4P\pi}{N}\right) \pm \cos\left(\frac{\pi}{\tau-1}\right) \right|}{\left| \sin\left(\frac{\pi}{\tau-1}\right) \right|},$$

with the lower sign corresponding to the first and the upper sign to the second quadrant of the upper half of the trigonometric circle. As  $m$  increases towards  $P$  we observe additional fluctuations resulting in a rather regular modulated pattern, containing a finite and small number of harmonic

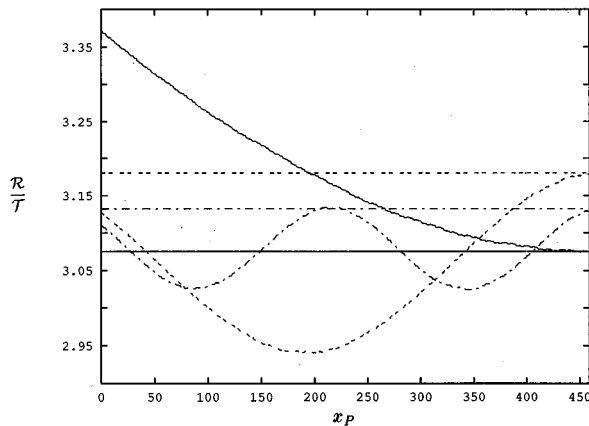


FIG. 7. Recurrence of simple behaviors as  $m$  crosses  $P$  (for  $N=2000$ , that yields  $P=472$  possible defect positions). Note a transition in the ordering of resistances between pure chains and ones with a defect: solid curves correspond to  $m=P$ ; dashed to  $m=P+1$ ; dot-dashed to  $m=P+2$ . (Flat lines always give the values of the corresponding chains *without* defect.)

modes (Fig. 6). The above mentioned “cycles” in the recurrence of the simplest behavior, occur whenever  $m$  approaches  $nP$  (again up to the symmetry around  $\phi_s = \pi/2$ ). As we cross the cycles we also observe abrupt changes of ordering in the resistance of the chain with the defect with respect to that of the pure chain (Fig. 7). Finally, close to the symmetry point  $\phi_s = \pi/2$  we observe largely fluctuating and modulated patterns that look self-similar [Figs. 8(a) and 8(b)]. These resistive patterns become chaotic [Fig. 8(c)] when we move sufficiently far from the special integrability points. [The above numerical observations are stable upon approaching the special point (i.e., decreasing  $\epsilon$ ) up to the lowest value of  $\epsilon$  where our convergence criterion is satisfied.]

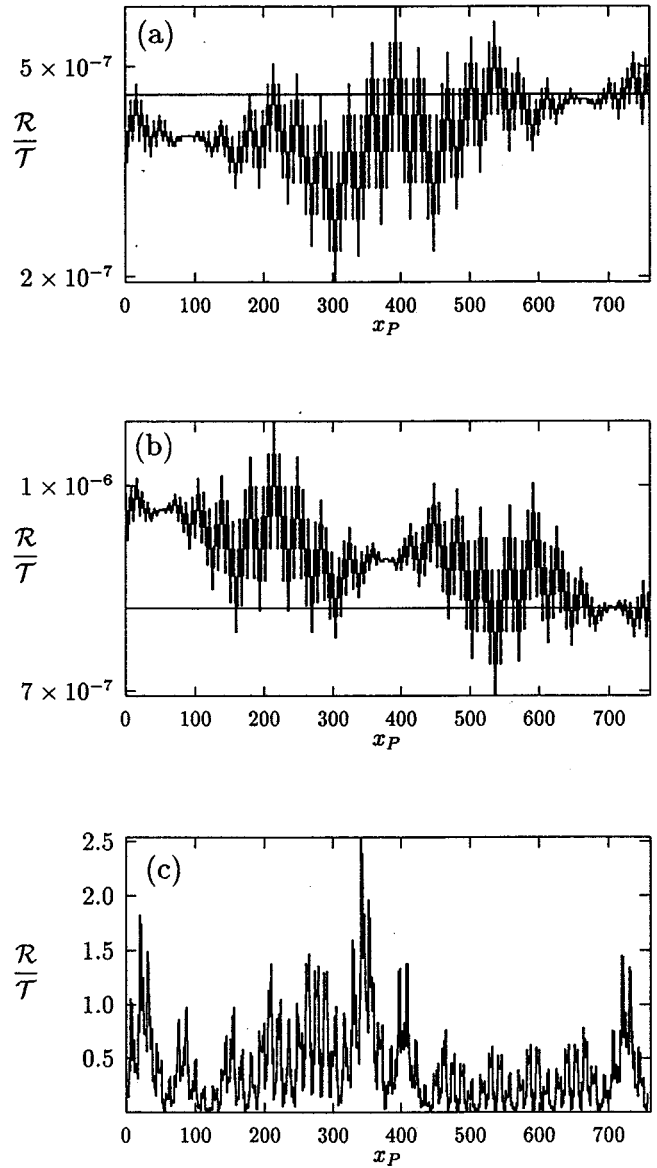


FIG. 8. Modulated and self-similar resistive patterns (close to special points) for chains with length  $N=3207$  (which yields  $P=757$  possible defect positions). (a) For  $m=1603$ , i.e., for  $\phi_s$  in the first quadrant and just before  $\pi/2$ . (b) For  $m=1605$ , i.e., for  $\phi_s$  in the second quadrant and two units after  $\pi/2$ . Both (a) and (b) are given for  $\epsilon=10^{-4}$ . (c) As  $\epsilon$  increases ( $\epsilon=0.5$ ) we recover chaotic behavior [the values of the parameters are the same as in case (b)].

We view the above results (summarized pictorially in Fig. 5) as interference effects between the abrupt “phase” change in hyperspace (that occurs at some point in physical space), and the phase of the wave function at that point. The Landauer resistance viewed as a function of the discrete variable  $x_p$  (that actually corresponds to a family of different physical systems) is here seen to carry a “memory” of the hyperspace by showing a type of “hypercoherence,” that depends on physical parameters in rather subtle ways.

#### IV. COMMENT ON INTRODUCTION OF FINITE TEMPERATURE $T$

The Landauer resistance at finite temperatures is given by<sup>20</sup>

$$\frac{\mathcal{R}}{\mathcal{T}}(T, \mu) = \frac{\int \left( -\frac{\partial f}{\partial E} \right) [1 - T(E)] dE}{\int \left( -\frac{\partial f}{\partial E} \right) T(E) dE}$$

with

$$f(E) = \frac{1}{1 + e^{\beta(E - \mu)}}, \quad \beta = \frac{1}{k_B T}.$$

For  $N \gg 1$  the transmission coefficients  $T(E)$ 's are dominant<sup>16</sup> in the local regions around the special points  $k_s$  (studied previously). Because of the smearing of the Fermi function at low temperatures, the behavior of the Landauer resistance with temperature depends on the location of the Fermi energy  $\mu$ . If  $\mu$  is close to a special energy (i.e., if  $\mu \sim \hbar^2 k_s^2 / 2m$ ) then the decrease or increase of  $\mathcal{R}/\mathcal{T}$  of the system with a defect compared to the pure system, depends on whether this particular  $k_s$  is a favorable or unfavorable point in the sense discussed on the previous pages. We conclude therefore, from our results above, that, statistically speaking, in the majority of cases the resistance will decrease upon increase of temperature.

#### V. CONCLUSIONS

Motivated by the anomalous transport properties of quasicrystals with defect and temperature, we have analyzed the role of phason defects on the Landauer resistance of a finite Fibonacci chain. In a tight-binding model with incident energy being fixed at the center of the band, the resistance is modified in an irregular fashion and in accordance with the behavior of the pure Fibonacci chain with the size of the system, with both positive and negative effect appearing statistically in equal percentage. In a fuller treatment of the continuous Schrödinger equation with  $\delta$ -function potentials, the modification of the resistance depends on the location of the Fermi level with respect to special energies corresponding to extended states, and also on the position of the defect. For finite chains, the majority of cases studied show a decrease of the Landauer resistance upon introduction of defect and temperature.

By comparing the two models, we have noted that continuous models, being free from truncation errors, preserve the phase coherence important for conductance and can reveal subtle additional effects. Such effects of interference between this coherence and the hyperspace construction have also been presented. It is interesting that most of the time, these give rise to exceedingly simple behaviors.

Although we do not study the thermodynamic limit with any rigor, the finite  $N$  results are *locally representative* because of the self-similarity in the resistance vs length behavior. Our focus on the local behaviors around the special conducting points  $k_s$  is justified by the fact that these are the only points relevant to conduction for  $N \gg 1$ , so that our results on resistance patterns should be representative for large systems. Some of these results could be tested experimentally in real chains that can be manufactured rather easily with recent advances in microfabrication techniques.<sup>21</sup>

#### ACKNOWLEDGMENT

One of us (K.M.) acknowledges support from the European Union through the Human Capital and Mobility Program.

<sup>1</sup>For a review, see C. Berger, in *Lectures On Quasicrystals*, edited by F. Hippert and D. Gratias (Les Editions de Physique Les Ulis, Aussois, France, 1994).

<sup>2</sup>T. Fujiwara, S. Yamamoto, and G. Trambly de Laissardiere, *Phys. Rev. Lett.* **71**, 4166 (1993).

<sup>3</sup>C. Janot, *Quasicrystals: A Primer*, 2nd ed. (Oxford Science, New York, 1994).

<sup>4</sup>M. Goda and H. Kubo, *J. Phys. Soc. Jpn.* **58**, 3624 (1989); H. Kubo and M. Goda, *ibid.* **60**, 2729 (1991); **62**, 2601 (1993); M. Goda and H. Kubo, *Mater. Sci. Forum* **150–151**, 179 (1994).

<sup>5</sup>M. Kohmoto, L. P. Kadanoff, and Ch. Tang, *Phys. Rev. Lett.* **50**, 1870 (1983); S. Ostlund, R. Pandit, D. Rand, H. J. Schellnhuber, and E. D. Siggia, *ibid.* **50**, 1873 (1983).

<sup>6</sup>This is not however true for smooth potentials. For example, if the strength of a smooth potential is small enough, the spectrum is absolutely continuous [see L. H. Eliasson, *Commun. Math.*

*Phys.* **146**, 447 (1992)], i.e., all states are extended.

<sup>7</sup>M. Kohmoto, *Phys. Rev. B* **34**, 5043 (1986); B. Sutherland and M. Kohmoto, *ibid.* **36**, 5877 (1987).

<sup>8</sup>M. Baake, D. Joseph, and P. Kramer, *Phys. Lett. A* **168**, 199 (1992).

<sup>9</sup>R. Landauer, *Philos. Mag.* **21**, 863 (1970).

<sup>10</sup>K. Mouloupoulos (unpublished).

<sup>11</sup>S. Roche (unpublished).

<sup>12</sup>A. Sanchez, E. Macia, and F. Dominguez-Adame, *Phys. Rev. B* **49**, 147 (1994).

<sup>13</sup>J. Bellissard, A. Formoso, R. Lima, and D. Testard, *Phys. Rev. B* **26**, 3024 (1982); J. B. Sokoloff and J. V. José, *Phys. Rev. Lett.* **49**, 334 (1982).

<sup>14</sup>E. Macia, F. D. Dominguez-Adame, and A. Sanchez, *Phys. Rev. B* **49**, 9503 (1994).

<sup>15</sup>R. de L. Krönig and W. G. Penney, in *Mathematical Physics in*

- One Dimension*, edited by E. H. Lieb and D. C. Mattis (Academic, New York, 1966), p. 243.
- <sup>16</sup>J. Kollar and A. Süto, Phys. Lett. A **117**, 203 (1986).
- <sup>17</sup>D. Würtz, M. P. Soerensen, and T. Schneider, Helv. Phys. Acta **61**, 345 (1988).
- <sup>18</sup>U. Thomas and P. Kramer, Int. J. Mod. Phys. B **3**, 1205 (1989).
- <sup>19</sup>M. Baake, U. Grimm, and D. Joseph, Int. J. Mod. Phys. B **7**, 1527 (1993).
- <sup>20</sup>H. L. Engquist and P. W. Anderson, Phys. Rev. B **24**, 1151 (1981).
- <sup>21</sup>R. Merlin *et al.*, Phys. Rev. Lett. **55**, 1768 (1985); J. Todd *et al.*, *ibid.* **57**, 1157 (1986).